ACI STRUCTURAL JOURNAL TECHNICAL PAPER

Title no. 101-S15

Compression Field Modeling of Reinforced Concrete Subjected to Reversed Loading: Verification

by Daniel Palermo and Frank J. Vecchio

General constitutive models for reinforced concrete subjected to reversed cyclic loading were recently developed for use in two-dimensional nonlinear finite element analyses, based on the smeared rotating crack assumption. The algorithm adopted was based on a total-load secant stiffness approach incorporating the compatibility, equilibrium, and constitutive relationships of the Modified Compression Field Theory (MCFT). Herein, verification is provided through analyses that include slender walls, which are controlled by flexural effects, and squat walls, where the response is dominated by shear-related mechanisms. The formulations are found to accurately simulate the behavior of structural walls, demonstrating that a secant stiffness procedure can effectively be adapted to model response to general loading. Behavioral aspects such as ultimate strength, ductility, energy dissipation, and failure mechanisms are well simulated. Second-order mechanisms are also examined and discussed, including the vertical elongation of flange walls and the in-plane horizontal expansion of central web walls, which affect the failure load and failure modes of structures. Shortcomings of the compression field approach are also addressed.

Keywords: cracks; loads; walls.

INTRODUCTION

Methods of analysis and modeling of concrete subjected to general loading conditions, including reversed cyclic loading, require improvement if the seismic response and ultimate strength of structures are to be evaluated with sufficient confidence. Procedures that provide adequate simulations of behavior under reversed cyclic loading conditions are less common than models applicable to monotonic loading. For such approaches, the smeared crack approach, assuming fixed cracks, tends to be the most favored. Okamura and Maekawa[1] and Sittipunt and Wood,[2] among others, have documented models assuming a fixed crack approach and have demonstrated reasonable agreement to experimental results. The fixed crack method requires separate formulations, however, to model the normal stress and shear stress hysteretic behavior. Rotating crack models, which alleviate the requirement to model normal stresses and shear stresses separately, are very popular for monotonic analyses. Examples of such formulations are those by Foster,[3] Ayoub and Filippou,[4] and Barzegar-Jamshidi and Schnobrich.[5] This approach, however, needs to be generalized to allow for cyclic load analyses and, thus, provide an alternative to the fixed crack model.

The alternate method suggested herein for reversed cyclic loading is based on smeared rotating cracks consistent with a compression field approach. The constitutive relations, recently reported by Palermo and Vecchio,[6] were formulated in the context of rotating cracks. The formulations were intended to improve upon preliminary models previously documented by Vecchio,[7] which demonstrated that a secant stiffness-based algorithm could be modified to provide accurate simulations of behavior for reversed cyclic loading conditions. Enhancements in the modeling include nonlinear unloading, degradation in the reloading stiffness based on the amount of strain recovered during unloading, improved modeling of plastic offsets, and partial unloading/reloading rules. Consideration was also given to the tension stress regime as it plays an important role in the overall behavior of reinforced concrete structures.

Presented herein are results of verification studies using a secant stiffness-based program employing the cyclic load formulations described in Reference 6. Structures considered include slender structural walls controlled by flexural effects and squat walls where the response is dominated by shear-related mechanisms.

RESEARCH SIGNIFICANCE

The state of the art in the analysis and modeling of reinforced concrete subjected to reversed loadings was brought into doubt as a result of the Seismic Shear Wall International Standard Problem documented by the Nuclear Power Engineering Corp. of Japan.[8] It became evident that calculating the peak strength of structural walls was not well established. More important, in the case of seismic analysis, was the apparent inability to accurately calculate structure ductility.

This paper provides verification for an alternate method of finite element analysis using constitutive relations formulated in the context of smeared rotating cracks, consistent with a compression field approach. The procedure provides accurate simulations of structural behavior including reversed cyclic loading.

FINITE ELEMENT IMPLEMENTATION

The cyclic load formulations documented by Palermo and Vecchio[6] were successfully implemented into an in-house nonlinear finite element program developed at the University of Toronto.[9] The program is a two-dimensional nonlinear finite element program, applicable to concrete membrane structures, that assumes rotating cracks. It is based on a secant stiffness formulation using a total-load, iterative procedure, employing the compatibility, equilibrium, and constitutive relations of the Modified Compression Field Theory (MCFT).[10] The reinforcement is typically modeled as smeared within the element but can also be discretely represented by truss bar elements. Further details are provided elsewhere.[9,11]

To perform a cyclic load analysis, the total concrete strain is separated into two components: an elastic strain and a plastic

ACI Structural Journal, V. 101, No. 2, March-April 2004.
MS No. 02-285 received August 9, 2002, and reviewed under Institute publication policies. Pertinent discussion including author's closure, if any, will be published in the January-February 2005 *ACI Structural Journal* if the discussion is received by September 1, 2004.

Daniel Palermo *is an NSERC postdoctoral fellow in the Department of Civil Engineering, McMaster University, Hamilton, Ontario, Canada. He received his PhD from the University of Toronto, Toronto, Ontario, Canada, in 2002. His research interests include nonlinear analysis and design of concrete structures, constitutive modeling of reinforced concrete subjected to cyclic loading, and large-scale testing and analysis of structural walls.*

Frank J. Vecchio, *FACI, is Professor and Associate Chair in the Department of Civil Engineering, University of Toronto. He is a member of Joint ACI-ASCE Committees 441, Reinforced Concrete Columns, and 447, Finite Element Analysis of Reinforced Concrete Structures. His research interests include nonlinear analysis and design of concrete structures, constitutive modeling, assessment, and repair and rehabilitation of structures.*

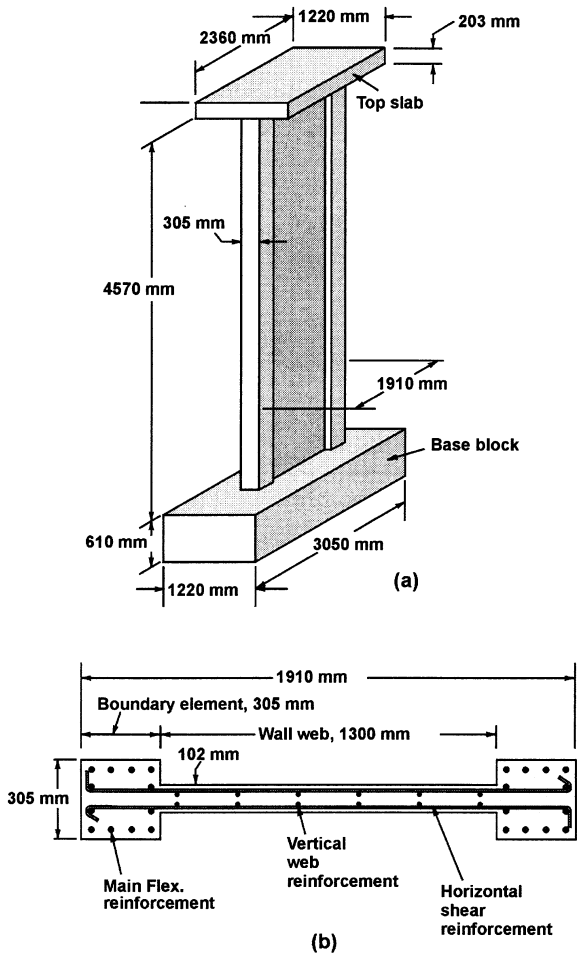

Fig. 1—Details of PCA walls, taken from Oesterle et al.[13]

strain. The elastic strain is used to compute an effective secant stiffness for the concrete, and the plastic strain, in turn, is treated as a strain offset, similar to an elastic offset as reported by Vecchio.[12] The plastic offsets are accommodated by resolving the plastic offsets in the principal directions into components relative to the reference axes. From the prestrains, free joint displacements are determined as functions of the element geometry. Then, plastic prestrain nodal forces can be evaluated using the effective element stiffness matrix due to the concrete component. The plastic offsets developed in each of the reinforcement components are also handled in a similar manner.

The total nodal forces for the element, arising from plastic offsets, are calculated as the sum of the concrete and reinforcement contributions. These are added to prestrain forces arising from elastic prestrain effects and nonlinear expansion effects. The analysis then proceeds as previously described.

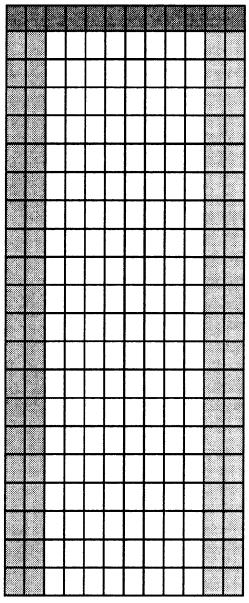

Fig. 2—Finite element mesh for PCA walls.

Vecchio[7] gives details describing the modifications for analysis capability of cyclic loading. The scope of this paper includes the verification of the cyclic models against structural walls available in the literature.

ANALYSIS OF SLENDER STRUCTURAL WALLS

First consider the series of walls tested by the Portland Cement Association (PCA),[13] consisting of 1/3-scale representations of a five-story wall. The Portland Cement Association specimens were barbell-shaped, measuring 1910 mm in total width and 4570 mm in height. The web walls were 102 mm thick and the boundary elements were 305 mm square. The specimens were built integral with a heavy base slab and stiff top slab. The PCA walls included in this investigation exhibited yielding of the flexural and vertical web reinforcement prior to failure, indicating that the response was dominated by flexural mechanisms prior to failure. Figure 1(a) illustrates the dimension details of a typical test specimen, and Fig. 1(b) depicts the typical reinforcement details.

Analyses were conducted on two representative PCA walls, B2 and B7, which provide a good test where crushing of concrete is preceded by the yielding of the flexural reinforcement. The test specimens were modeled using the finite element mesh shown in Fig. 2, which consisted of 252 constant-strain rectangular elements. The mesh was divided into three zones, representing the web portion, the flanges (boundary elements), and the top slab. For analysis purposes, the bottom slab was omitted and the wall was assumed fully fixed at the base. The top slab was modeled as a stiff element through which loading was transferred to the wall section. The material properties and reinforcement details used in the modeling, listed in Table 1, were as reported by Sittipunt and Wood.[2] Note that boundary elements of Specimen B7 were confined with tie reinforcement.

Loading, consisting of predetermined lateral displacements, was imposed along the top stiff slab in increments of 25 mm and included two repetitions. Axial loading of approximately 3.77 MPa was imposed on Wall B7; otherwise, the two test specimens were subjected to similar loading conditions.

The observed and calculated load-deformation responses for Specimen B2 are shown in Fig. 3(a) and (b), respectively.

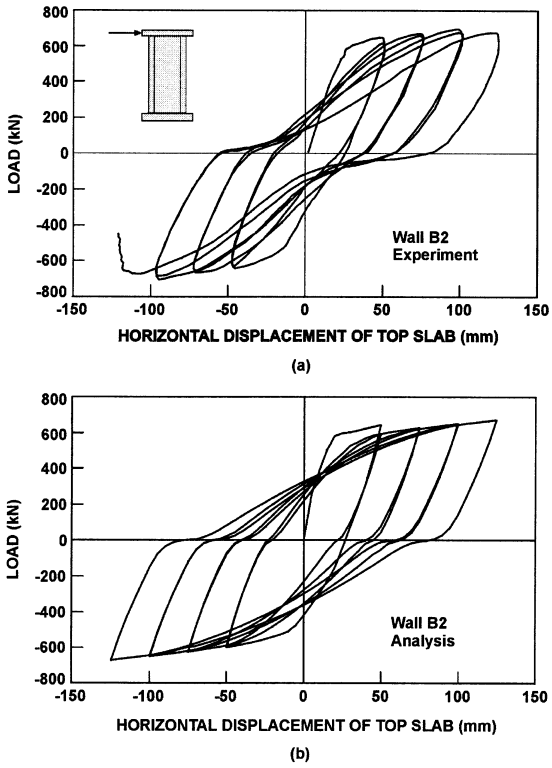

Fig. 3—Load-deformation responses of B2: (a) observed, taken from Oesterle et al.;[13] and (b) calculated.

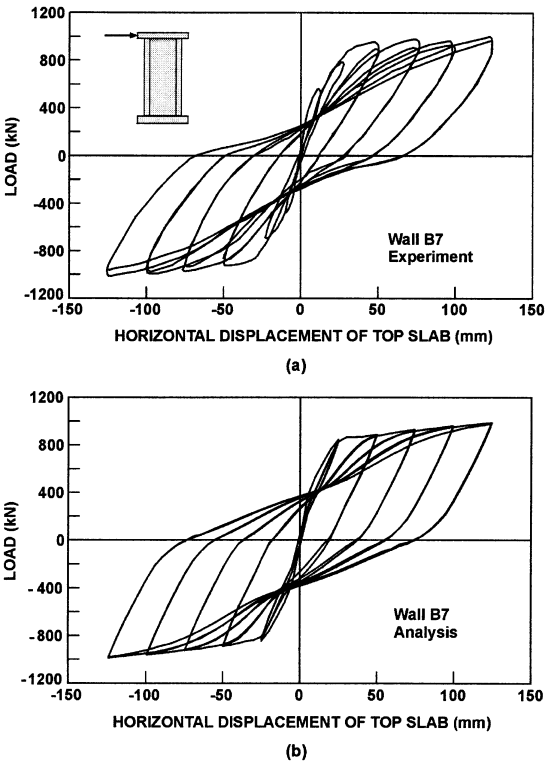

Fig. 4—Load-deformation responses of B7: (a) observed, taken from Oesterle et al.;[13] and (b) calculated.

Figure 4(a) and (b) illustrate the experimental and simulated results of Wall B7, respectively. Relative to the measured response, the analyses compute the ultimate lateral resistance, residual displacements, precracking and postcracking stiffness, and energy dissipation reasonably well. The near flat-top behavior, typical of flexure-dominant mechanisms, is also captured by the analyses. The one notable discrepancy between the calculated and observed behaviors is the degree of pinching and, to a lesser extent, the slight underestimation of the degradation in the reloading stiffness of the second excursion of each displacement level. This anomaly seems to be a function of overestimating the strains in the longitudinal reinforcement. Vecchio[14] recently described a refinement to the MCFT, known as the Disturbed Stress Field Model (DSFM), that addresses discontinuous crack shear slip. Generally, the DSFM results in less straining in the longitudinal reinforcement relative to the MCFT, resulting in more pinching in the hysteresis response.

The finite element analyses calculated lateral resistances similar to those observed. For B2, a load of 671 kN was calculated at 125 mm of lateral displacement, compared with a measured resistance of 710 kN at 100 mm. A lateral resistance of 995 kN was calculated for B7, while the observed load was 1025 kN, both occurring at 150 mm of displacement.

Failure of Walls B2 and B7, as reported by Sittipunt and Wood,[2] was observed during the first excursion to –125 and +150 mm, respectively, and ultimately involved crushing of the concrete in the web wall. Note that the near flat-top response and significant residual displacements indicate that yielding of the vertical reinforcement preceded crushing of the concrete. The analyses did not capture a sudden failure as observed; however, based on significant indicators from the finite element analyses, the walls were experiencing significant damage throughout. The analyses indicated extensive crushing and excessive yielding of the vertical reinforcement

Table 1—Material properties for PCA wall series

		Concrete		Reinforcement					
				Horizontal		Vertical		Confining	
Specimen	Zone	f'_c, MPa	E_c, MPa	ρ, %	f_y, MPa	ρ, %	f_y, MPa	ρ, %	f_y, MPa
B2	Web	53.6	32,700	0.63	532	0.29	532	—	—
	Boundary	53.6	32,700	0.63	532	3.67	410	—	—
B7	Web	49.3	30,100	0.63	489	0.29	489	—	—
	Boundary	49.3	30,100	0.63	489	3.67	457	1.35	489

over the bottom third of the wall. Yielding of the horizontal reinforcement was also calculated throughout the web. Essentially, the analysis results of B2 and B7 indicated failure due to crushing of the concrete in the web. Results of analyses conducted on other PCA walls can be found elsewhere.[15]

Further corroboration involves the SW series of wall tests conducted by Pilakoutas and Elnashai.[16] The SW specimens investigated were rectangular in shape (1200 mm high, 600 mm long, and 60 mm thick). The walls also contained concealed columns at the ends of the wall. Walls SW4 and SW6 are discussed herein; detailed results and analyses on other SW walls can be found in Reference 15. The walls demonstrated slight differences in the load-deformation response and in the failure mechanisms, thus providing a challenging set of tests to the cyclic models employed in the analyses. The dimensional details and a typical reinforcement layout are shown in Fig. 5(a) and (b), respectively.

The finite element mesh used in the modeling, shown in Fig. 6, comprised of 117 constant-strain rectangular elements, was divided into a web zone, a boundary element zone, and a top slab. The base slab was omitted, and the wall was assumed fully fixed at the base. Table 2 contains the material properties and reinforcement details of SW4 and SW6.

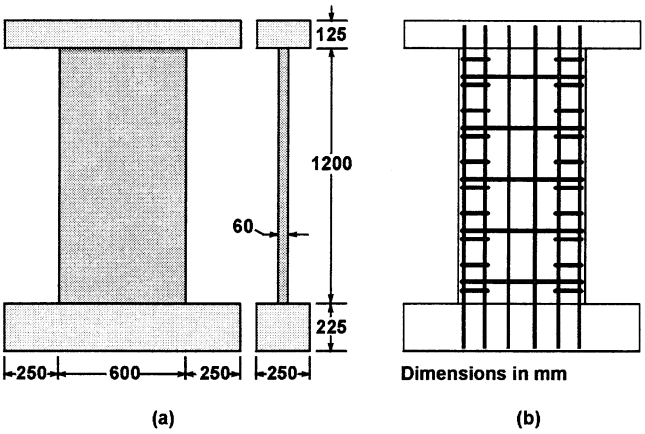

Fig. 5—Details of SW walls: (a) dimensions; and (b) typical reinforcement layout.

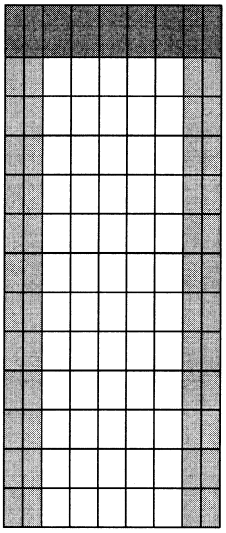

Fig. 6—Finite element mesh for SW walls.

Table 2—Material properties for SW wall series

Specimen	Zone	Concrete		Reinforcement					
				Horizontal		Vertical		Confining	
		f'_c, MPa	E_c, MPa	ρ, %	f_y, MPa	ρ, %	f_y, MPa	ρ, %	f_y, MPa
SW4	Web	37.0	35,240	0.39	545	0.50	545	—	—
	Boundary	37.0	35,240	0.79	545	6.86	470	0.43	545
SW6	Web	38.6	36,075	0.31	400	0.50	545	—	—
	Boundary	38.6	36,075	0.31/ 0.66*	400	6.86	470	0.0/ 0.19*	400

*Represents reinforcement in bottom half of boundary elements.

Specimen SW6 contained less shear reinforcement, and the confining reinforcement was concentrated in the bottom half of the boundary elements; otherwise the properties were similar to SW4. The loading history involved increasing lateral cyclic displacements imposed on the top slab in increments of 2 mm until failure, with two excursions per displacement level.

The observed load-deformation response of SW4, shown in Fig. 7(a), provides a good test where significant yielding of the flexural reinforcement precedes failure, as is evident from the near flat-top response. Note that the second excursion of loading has been omitted for clarity. The calculated finite

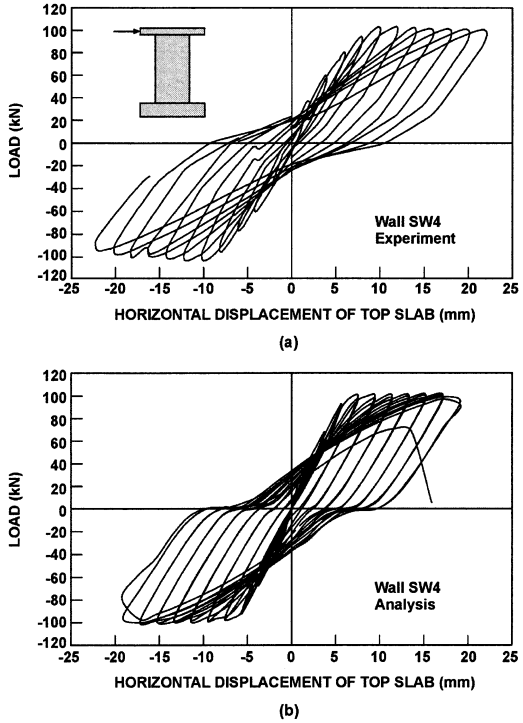

Fig. 7—Load-deformation responses of SW4: (a) observed, taken from Pilakoutas and Elnashai;[16] and (b) calculated.

element response, shown in Fig. 7(b), simulated the overall behavior exceptionally well. The rounded experimental response of test Specimen SW6, shown in Fig. 8(a), seems more influenced by the behavior of the concrete and provides a more stringent test for the unloading/reloading formulations for the concrete used in the analysis. The calculated response in Fig. 8(b) reasonably captures the overall behavior; relative to the observed behavior, however, the simulation is characterized by a flat-top response. As previously described, this is a result of calculating larger strains in the longitudinal reinforcement, which has recently been addressed by the DSFM.

Generally, the analyses of SW4 and SW6 sufficiently simulated the peak strengths, residual displacements, pinching of the hysteresis loops, energy dissipation, and observed failure mechanisms. The experimental lateral resistance of SW4 was realized at 10 mm of displacement and measured 104 kN. The analyses indicated a maximum calculated resistance of 100 kN at 10 mm of lateral displacement. Failure was calculated at 22 mm of displacement and involved crushing of the concrete at the boundary elements, followed by the formation of a sliding shear plane. Significant yielding of the flexural reinforcement and substantial horizontal expansion of the wall were also calculated prior to failure. The only notable difference was that failure was observed at 24 mm of displacement during testing; otherwise, the calculated failure mechanism was consistent with the observed behavior.

Similar results were obtained with test Specimen SW6. An observed maximum lateral resistance of 108 kN was reported, corresponding to a displacement of 18 mm. The analyses indicated a peak calculated resistance of 102 kN; however, the corresponding lateral displacement was 10 mm. This does not necessarily suggest that the calculated displacement was grossly in error. The analysis produced a near flat-top response, and very little difference in loads was calculated for lateral displacements in the 10 to 20 mm range. The failure mechanism

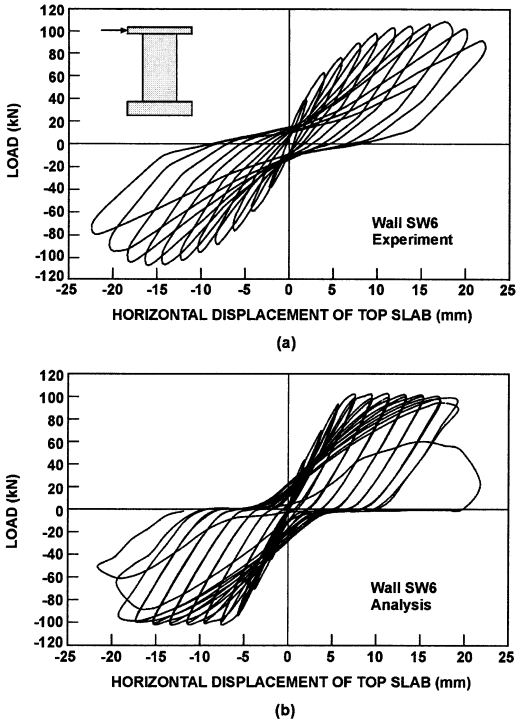

Fig. 8—Load-deformation responses of SW6: (a) observed, taken from Pilakoutas and Elnashai;[16] and (b) calculated.

was accurately captured by the finite element analysis and eventually involved a sliding shear plane near the base of the wall, preceded by crushing of the concrete near the base of the boundary elements and yielding of the flexural and horizontal reinforcement. The observed failure ultimately occurred as a result of opening of the diagonal cracks, which was captured in the analysis by calculating significant horizontal expansion of the wall.

The PCA and SW series of structural walls have long been considered benchmarks against which theoretical calculations can be calibrated. The walls are dominated by flexural mechanisms; thus, yielding of the reinforcement significantly controls the response. The overall behavior, therefore, is only marginally affected by the choice of a cyclic model for the concrete. The reinforcement model implemented in the finite element analysis, adopted from Seckin,[17] is commonly accepted among researchers and is well understood. To better test constitutive formulations of the concrete, squat structural walls more heavily influenced by shear-related mechanisms must be investigated. The response of squat walls is significantly influenced by the concrete behavior and will be discussed in more detail in subsequent sections. Nonetheless, the analytical results indicate that the proposed cyclic models are capable of describing the response of flexure-dominant structures.

ANALYSIS OF SQUAT STRUCTURAL WALLS

The DP experimental program[18] was intended to complement the current body of data in the literature with data from squat walls more heavily influenced by shear-related mechanisms. Such mechanisms place more demand on the concrete, and failure is quite often associated with shear crushing of the concrete. The DP walls experienced extensive crushing of the concrete throughout the central web wall, while yielding of the reinforcement seemed to be confined locally at cracks. The two specimens of interest here are DP1 and DP2: two

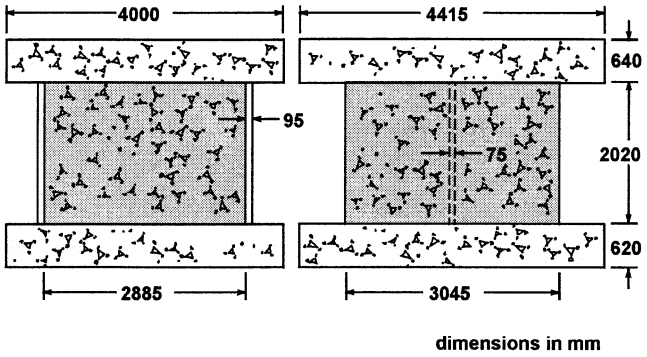

Fig. 9—Details of DP walls, taken from Palermo and Vecchio.[18]

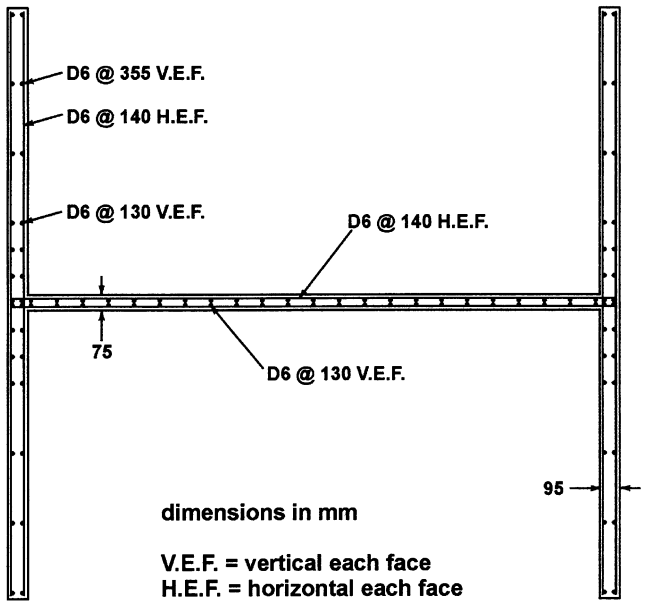

Fig. 10—Reinforcement layout of DP walls, taken from Palermo and Vecchio.[18]

large-scale flanged reinforced walls that were constructed with stiff top and bottom slabs. The top slab (4415 x 4000 x 640 mm) served to distribute the horizontal and axial loads to the walls of the structure. The bottom slab (4415 x 4000 x 620 mm), clamped to the laboratory strong floor, simulated a rigid foundation. The slabs were reinforced with No. 30 deformed reinforcing bars at a spacing of 350 mm in each direction, with a top and bottom layer. The web wall, 2885 mm in length, 2020 mm in height, and 75 mm in thickness, was reinforced with D6 reinforcing bars. The bars were spaced 140 mm horizontally and 130 mm vertically in two curtains. The two flange walls were approximately 3045 mm long, 2020 mm high, and 95 mm thick for DP1 and 100 mm thick for DP2. The flanges were also reinforced with D6 reinforcing bars, spaced 140 mm horizontally. The bars were spaced vertically at 130 mm near the web wall and 355 mm near the tips of the flanges. Dimensional details and a sectional view of the reinforcement layout of the walls are shown in Fig. 9 and 10, respectively.

The finite element mesh, shown in Fig. 11, consisted of 540 constant-strain rectangular elements. Given that the finite elements in the analysis package are low-powered, mesh refinement becomes critical if important structural behaviors are to be properly simulated. The mesh selected for the analyses provided a compromise between being able to capture

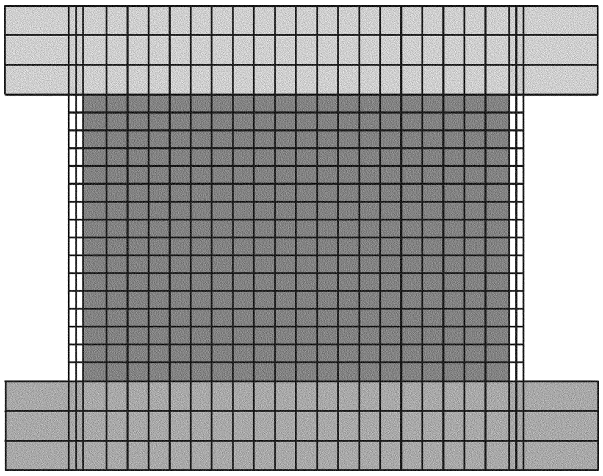

Fig. 11—Finite element mesh for DP walls, taken from Palermo and Vecchio.[18]

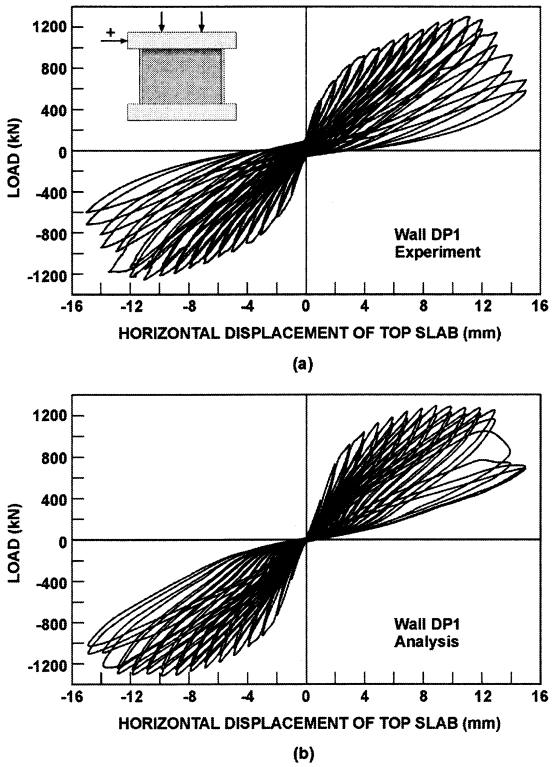

Fig. 12—Load-deformation responses of DP1: (a) observed, taken from Palermo and Vecchio;[18] and (b) calculated.

important phenomena and the insignificant return of further refinement. Vecchio[19] conducted a parametric study on mesh size using the Nuclear Power Engineering Corporation of Japan's structural walls, which were similar to the DP test specimens. The investigation considered improvements in behavior with mesh refinement.

The mesh was divided into four zones: the web wall, flange walls, and top and bottom slabs. The base slab was assumed fully fixed to the laboratory strong floor. The full width of the flanges, assumed to be fully effective in contributing to the lateral load resistance, was concentrated into a single element in the two-dimensional model. Table 3 contains the material properties and reinforcement details of DP1 and DP2. The only notable difference is the concrete compressive cylinder strength of the walls.

Table 3—Material properties for DP wall series

Specimen	Zone	Concrete		Reinforcement			
				Horizontal		Vertical	
		f'_c, MPa	E_c, MPa	ρ, %	f_y, MPa	ρ, %	f_y, MPa
DP1	Web	21.7	25,900	0.74	605	0.79	605
	Boundary	21.7	25,900	0.58	605	0.63/ 0.23*	605
DP2	Web	18.8	18,580	0.74	605	0.79	605
	Boundary	18.8	18,580	0.58	605	0.63/ 0.23*	605

*0.23% represents reinforcement near flange tips.

Loading was imposed on the top slab and involved reversed cyclic horizontal displacements in increments of 1 mm until failure. Two repetitions of loading were applied at each displacement level. Additionally, an externally applied axial load of 940 kN was introduced to the top slab of Specimen DP1. The analyses also accounted for the 260 kN self-weight of the top slab for DP1 and DP2. A shrinkage strain of -0.4×10^{-3}, significant to the finite element analyses, was included in the loading. The shrinkage accounts for the delay in testing from the time of casting and has the effect of causing tensile stresses in the concrete, which leads to cracking and a reduction in the stiffness of the structure. For DP1, 183 days had passed between casting and the start of testing, and for DP2, the delay had spanned 168 days.

The experimental and simulated results of the lateral load versus the horizontal displacement of the top slab for DP1 are shown in Fig. 12(a) and (b), respectively. The observed response, discussed in detail in Reference 18, is typical of shear-dominant behavior. The hysteresis loops are highly pinched, and the energy dissipation is insignificant in comparison to that observed in walls with flexure-dominant responses. Also evident is the degradation of the reloading stiffness during the second excursion for each displacement level, becoming more pronounced in the postpeak range.

The analyses, in general, simulated the lateral resistance, ductility, residual displacements, and energy dissipation exceptionally well. More specifically, the postpeak response, the progressive degradation in the reloading stiffness, and the damage experienced during the second excursion of displacement were successfully captured. The maximum lateral strength was calculated more accurately than the corresponding displacement. The analysis estimated a resistance of 1307 kN at a displacement of 9.87 mm, whereas a strength of 1298 kN corresponding to a displacement of 11.14 mm was reported during testing.

The cyclic models used in the finite element analysis calculated a failure mechanism consistent with the observed behavior. The web wall experienced extensive crushing throughout, followed by the formation of five vertical slip planes by the end of the analysis. No yielding of the flange flexural or web horizontal reinforcement was calculated; however, there was some local yielding of the vertical web reinforcement. The vertical slip planes were first calculated at 10 mm of displacement and formed near the flange walls. All of these aspects of behavior were similar to the observed behavior. The only discrepancy was the presence of an additional slip plane in the observed failure. Figure 13(a) and (b) illustrate the observed and simulated state of failure for Specimen DP1, respectively.

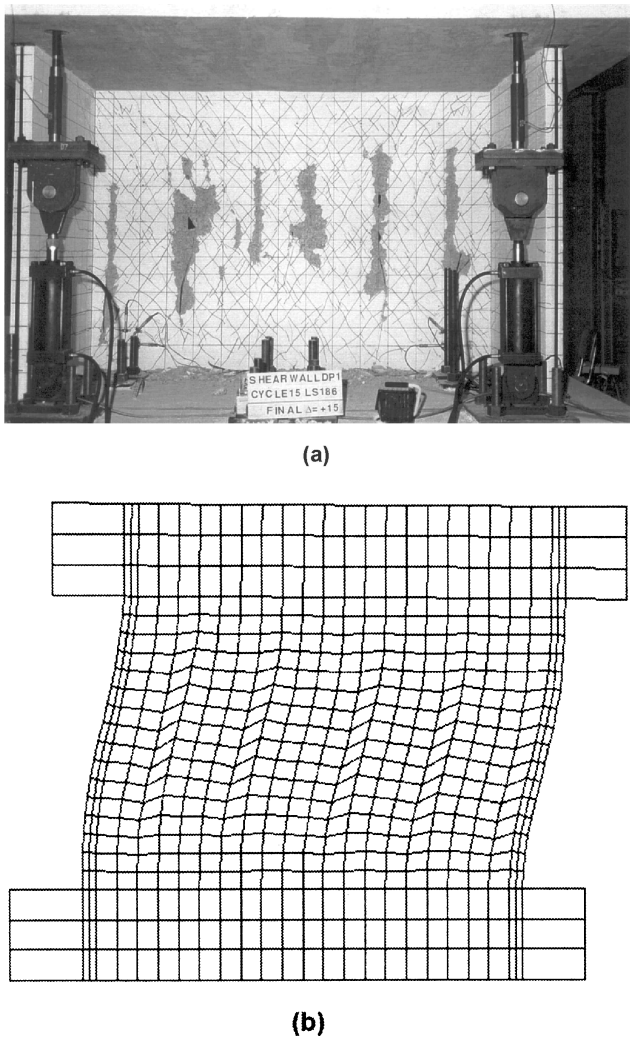

Fig. 13—Failure mechanisms of DP1: (a) observed, taken from Palermo and Vecchio;[18] and (b) calculated.

A subsequent analysis was performed on Specimen DP2. The observed and simulated lateral load-deformation responses are illustrated in Fig. 14(a) and (b), respectively. Similar to DP1, Specimen DP2 also demonstrated shear-dominant characteristics including: significantly pinched hysteresis loops, small residual displacements, and marginal energy dissipation. Note that the observed response did not realize a postpeak behavior, as a sudden loss of capacity followed the maximum lateral resistance.

The calculated response captured the behavior of DP2 reasonably well up to 9 mm of displacement including: the energy dissipation through hysteresis, the residual displacements, and the lateral load at each displacement level. Further, the degradation in the reloading stiffness for the second repetition of loading was also simulated successfully. Specimen DP2, however, failed abruptly during loading to 10 mm of displacement. This failure seemed to be the result of weaker concrete near the top of the walls. (Refer to Reference 18 for more details of the mechanisms leading to failure.) A more appropriate assessment would be to compare the results at 9 mm of displacement (the last load stage before the observed failure). The analysis calculated a lateral resistance of 969 kN at a corresponding displacement of 8.86 mm, whereas the test results indicated a wall strength of 904 kN at a displacement of 9.15 mm.

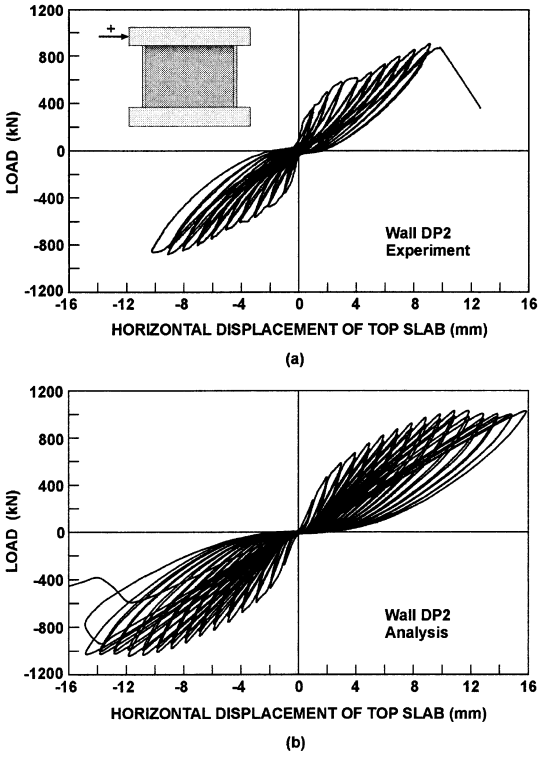

Fig. 14—Load-deformation responses of DP2: (a) observed, taken from Palermo and Vecchio;[18] and (b) calculated.

The initial analysis, which assumed a constant concrete strength throughout the walls, calculated a sliding shear failure 375 mm from the base slab, occurring during loading to the second excursion to 15 mm of displacement. Vertical crushing planes were also evident in the positive loading direction at failure. Yielding of the horizontal reinforcement in the web wall and local yielding of the flange flexural reinforcement preceded failure. Figure 15(a) and (b) depict the observed and calculated modes of failure, respectively. Note the sliding shear plane near the top slab of the observed failure.

A further analysis was conducted on DP2 to investigate the failure mechanism. As noted previously, it has been suggested[18] that weaker concrete in the wall sections near the top slab was a probable cause of failure. In the second analysis, the concrete compressive strength, determined from standard cylinders, in the top four rows of elements in the web and flange zones was reduced by 30%. The reduction was also applied to the initial concrete stiffness and the tensile cracking strength. All other material properties and loading conditions remained unchanged. The load-deformation results are given in Fig. 16, and Fig. 17 illustrates the calculated state of the structure at failure.

The modified analysis calculated an abrupt failure during loading to 12 mm of displacement, following attainment of a maximum resistance of 983 kN during loading to 11 mm. Similar to the observed behavior, a sliding shear failure was calculated at approximately 375 mm from the top slab. Yielding of the horizontal web reinforcement was calculated after the formation of the sliding shear plane. Crushing of the concrete in the compression toes near the base slab was also calculated at 6 mm of lateral displacement. These damage indicators were consistent with the observed behavior. A further reduction in the compressive strength of the concrete would result in an indicated failure at smaller displacements in the web wall near the top slab. Therefore, it appears that

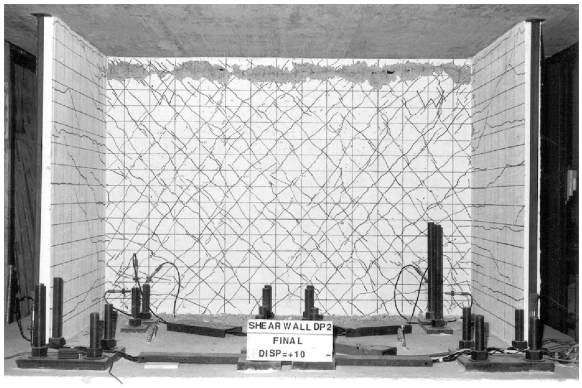

(a)

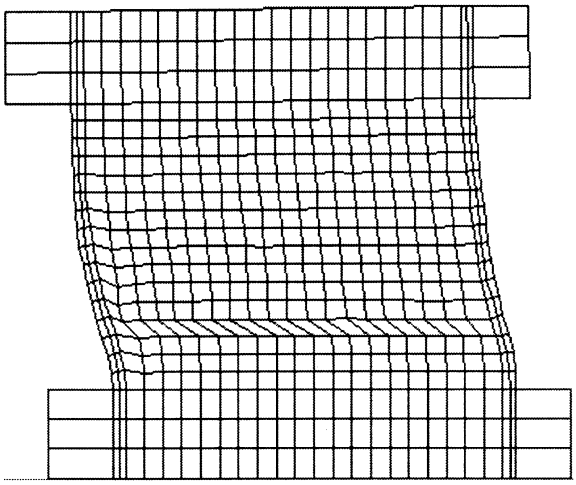

(b)

Fig. 15—Failure mechanisms of DP2: (a) observed, taken from Palermo and Vecchio;[18] and (b) calculated.

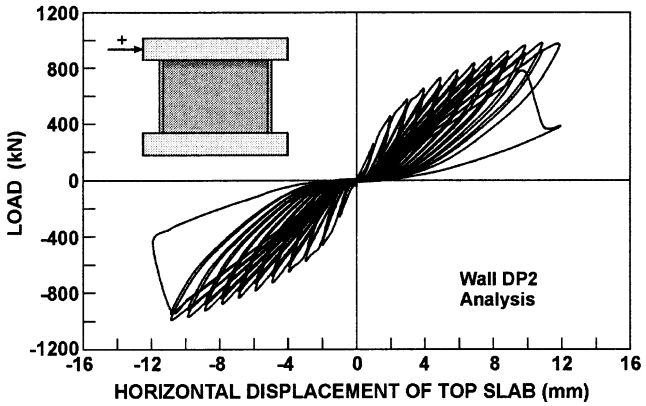

Fig. 16—Modified load-deformation response of DP2.

weaker concrete in the upper part of the walls was a probable cause for the sudden sliding shear failure near the top slab.

The analyses of the three sets of wall tests reveal some interesting observations regarding modeling of concrete subjected to reversed cyclic loading. Where the actual behavior is flexure-dominant and yielding of the reinforcement precedes failure, the overall load-displacement response appears to be unaffected by the choice of unloading/reloading rules for concrete. This was evident in the analyses conducted on the PCA and SW series of structural walls. However, where shear is the dominant mechanism, and the concrete experiences

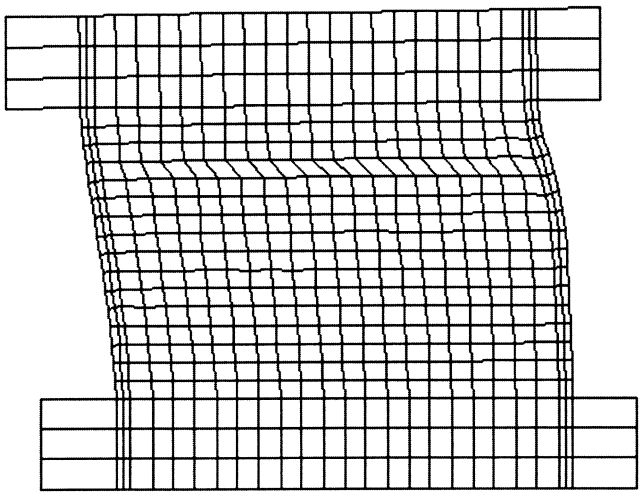

Fig. 17—Modified failure mechanisms of DP2.

significant damage prior to yielding of the reinforcement, the concrete cyclic models become critical if the overall behavior and, more importantly, the failure mechanisms are to be accurately simulated. Even though the selection of concrete cyclic models may not influence the macroscopic behavior of flexure-dominant walls, it is significant in correctly calculating localized damage, failure modes, and failure loads.

SECOND-ORDER MECHANISMS

Test data that are particularly useful in understanding behavior and corroborating analytical models are those of a second-order nature, describing subtleties in response. Among them is the elongation of the flange wall, which is a measure of the extent of flexural cracking and the ratcheting in the flange walls. (Ratcheting is a term used to describe the vertical stretching of the flange due to irrecoverable strains that accumulate in the postyield cycles.) Figure 18(a) and (b) illustrate the observed and simulated elongation of the flange walls for Specimen DP1. The experimental response for DP2 can be found elsewhere.[18]

Note that in the observed response, as the stiffness diminishes with increased lateral displacement, there is some accumulation in the residual displacement. The effect is minor and suggests that yielding of the reinforcement was minimal. Less evident is the diminishing elongation of the flange wall in the post-peak range, also suggesting that yielding was insignificant. The calculated response demonstrates reasonable simulation of the flange wall elongation. This includes: the overall behavior, stiffness, hysteresis loops, degradation of the reloading path during the second repetition of displacement, and the recovery of the vertical stretching in the postpeak region. The only notable difference is the calculated degree of pinching. This seems to indicate a slight deficiency in the MCFT, which is based on average strains and stresses in the reinforcement. Thus, yielding of the reinforcement is assumed only when the average strain reaches the yield strain, even though yielding initially occurs locally at cracks. The condition of the reinforcement at the cracks contributes to the accumulation of the residual displacements and requires further investigation.

A maximum vertical elongation of 3.6 mm during loading to 13 mm of lateral displacement was calculated by the finite element analysis, compared with the observed elongation of 4.2 mm attained at 12 mm of displacement. Bond slip near

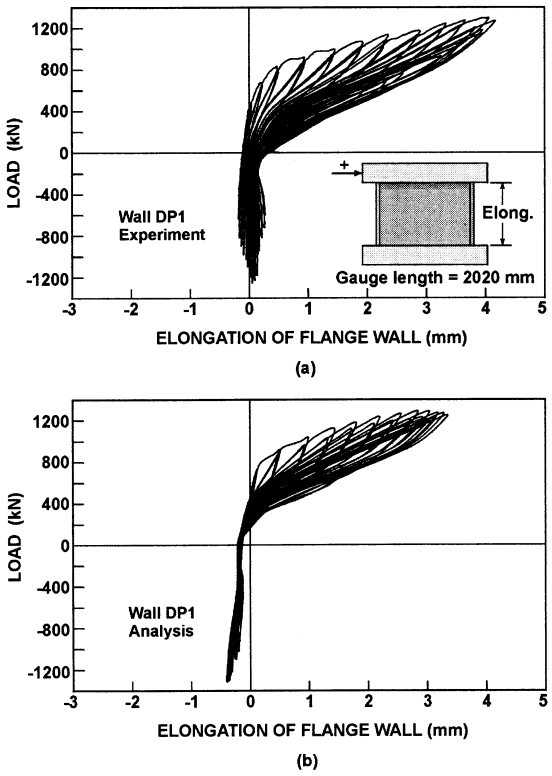

Fig. 18—Elongation of flange wall for Specimen DP1: (a) observed, taken from Palermo and Vecchio;[18] and (b) calculated.

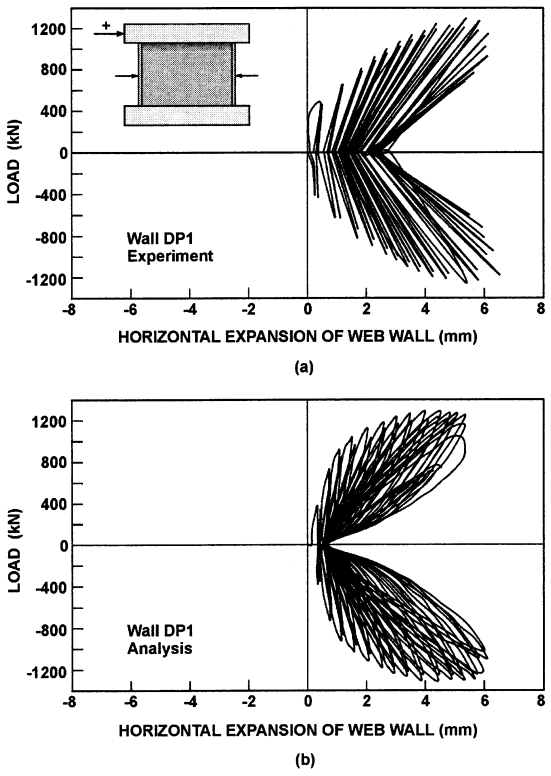

Fig. 19—Horizontal expansion of web wall for Specimen DP1: (a) observed; and (b) calculated.

the base of the wall, neglected in the analysis, was a probable factor contributing to the discrepancy.

Another important second-order mechanism is the horizontal expansion of the web wall at midheight. The expansion is a measure of the dilation of the web wall due to cracking and yielding of the web reinforcement. It also indicates the extent of compression softening of the concrete in the web wall. Capturing this behavior is critical to accurately calculating the load capacity and failure mode of the structure.[19] The observed and calculated responses for DP1 are illustrated in Fig. 19(a) and (b), respectively. (Note: A continuous response for Fig. 19(a) was not available during testing, and expansion values at maximum and zero loads are plotted for each displacement level.)

The increasing horizontal expansion of the web wall beyond the postpeak load stages, in addition to the accumulating residual displacements, suggests that yielding of the web reinforcement was prevalent. Not withstanding the residual displacements, the simulated response reasonably captured all aspects of behavior. As previously suggested, the underestimation of the residual displacements seems to be a slight deficiency in the MCFT approach in handling local reinforcement strains.

The finite element analysis calculated a maximum horizontal expansion of 6.1 mm during loading to 15 mm of lateral displacement, whereas the observed expansion of 6.5 mm was reported at 13 mm of displacement. Experimental results of DP2 can be found in Reference 18.

CONCLUSIONS

Constitutive models for reinforced concrete subjected to reversed cyclic loading were recently developed;[6] this paper has provided verification and validation of those models.

Based on comprehensive nonlinear finite element analyses of various structural walls, the following conclusions are derived:

1. Smeared rotating crack formulations can be adapted to provide a platform for cyclic load analyses;
2. The MCFT/DSFM, with the proposed constitutive models, produce simple and accurate simulations of behavior in cyclically loaded structural walls;
3. It is possible and important to capture subtle second-order behavior mechanisms as well as general overall load-deformation response;
4. The analyses indicated that slender walls, controlled by flexural mechanisms, are generally a test for reinforcement models, whereas squat walls, demonstrating shear-dominant behavior, are a better test for concrete models; and
5. In cyclic load analyses, it is important to capture local conditions at cracks. Local yielding and accumulation of reinforcing bar strains at cracks are particularly important. Imperfect crack closing is also a significant factor. Further studies are required to address these shortcomings.

NOTATION

E_c = initial modulus of concrete
f'_c = peak compressive strength of concrete cylinder
f_y = yield stress of reinforcement
ρ = reinforcement ratio

REFERENCES

1. Okamura, H., and Maekawa, K., *Nonlinear Analysis and Constitutive Models of Reinforced Concrete*, Giho-do Press, University of Tokyo, 1991, 182 pp.

2. Sittipunt, W., and Wood, S. L., "Influence of Web Reinforcement on the Cyclic Response of Structural Walls," *ACI Structural Journal*, V. 92, No. 6, Nov.-Dec. 1995, pp. 745-756.

3. Foster, S. J., "The Structural Behavior of Reinforced Concrete Deep Beams," PhD thesis, University of New South Wales, New South Wales, Australia, 1992.

4. Ayoub, A., and Filippou, F. C., "Nonlinear Finite Element Analysis of RC Shear Panels and Walls," *Journal of Structural Engineering*, ASCE, V. 124, No. 3, 1998, pp. 298-308.

5. Barzegar-Jamshidi, F., and Schnobrich, W. C., "Nonlinear Finite Element Analyses of Reinforced Concrete Under Short-Term Monotonic Loading," *Civil Engineering Studies Report* No. 530, University of Illinois at Urbana-Champaign, Ill., 1986.

6. Palermo, D., and Vecchio, F. J., "Compression Field Modeling of Reinforced Concrete Subjected to Reversed Loading: Formulation," *ACI Structural Journal*, V. 100, No. 5, Sept.-Oct. 2003, pp. 616-625.

7. Vecchio, F. J., "Towards Cyclic Load Modeling of Reinforced Concrete," *ACI Structural Journal*, V. 96, No. 2, Mar.-Apr. 1999, pp. 193-202.

8. Nuclear Power Engineering Corporation of Japan (NUPEC), "Comparison Report, Seismic Shear Wall ISP, NUPEC's Seismic Ultimate Dynamic Response Test," *Report* No. NU-SSWISP-D014, Organization for Economic Co-Operation and Development, Paris, 1996, 407 pp.

9. Vecchio, F. J., "Nonlinear Finite Element Analysis of Reinforced Concrete Membranes," *ACI Structural Journal*, V. 86, No. 1, Jan.-Feb. 1989, pp. 26-35.

10. Vecchio, F. J., and Collins, M. P., "The Modified Compression-Field Theory for Reinforced Concrete Elements Subjected to Shear," ACI JOURNAL, *Proceedings* V. 83, No. 2, Mar.-Apr. 1986, pp. 219-231.

11. Vecchio, F. J., "Reinforced Concrete Membrane Element Formulations," *Journal of Structural Engineering*, ASCE, V. 116, No. 3, 1990, pp. 730-750.

12. Vecchio, F. J., "Finite Element Modeling of Concrete Expansion and Confinement," *Journal of Structural Engineering*, ASCE, V. 118, No. 9, 1992, pp. 2390-2406.

13. Oesterle, R. G.; Fiorato, A. E.; Johal, L. S.; Carpenter, J. E.; Russell, H. G.; and Corley, W. G., "Earthquake-Resistant Structural Walls—Tests of Isolated Walls," *Report* to National Science Foundation, Construction Technology Laboratories, Portland Cement Association, Skokie, Ill., 1976, 315 pp.

14. Vecchio, F. J., "Disturbed Stress Field Model for Reinforced Concrete: Formulation," *Journal of Structural Engineering*, ASCE, V. 126, No. 9, 2000, pp. 1070-1077.

15. Palermo, D., and Vecchio, F. J., "Behavior and Analysis of Reinforced Concrete Walls Subjected to Reversed Cyclic Loading," *Publication* No. 2002-01, Department of Civil Engineering, University of Toronto, Toronto, Ontario, Canada, 2002, 351 pp.

16. Pilakoutas, K., and Elnashai, A., "Cyclic Behavior of Reinforced Concrete Cantilever Walls, Part I: Experimental Results," *ACI Structural Journal*, V. 92, No. 3, May-June 1995, pp. 271-281.

17. Seckin, M., "Hysteretic Behaviour of Cast-in-Place Exterior Beam-Column Sub-Assemblies," PhD thesis, University of Toronto, Toronto, Ontario, Canada, 1981, 266 pp.

18. Palermo, D., and Vecchio, F. J., "Behavior of Three-Dimensional Reinforced Concrete Shear Walls," *ACI Structural Journal*, V. 99, No. 1, Jan.-Feb. 2002, pp. 81-89.

19. Vecchio, F. J., "Lessons From the Analysis of a 3-D Concrete Shear Wall," *Structural Engineering and Mechanics*, V. 6, No. 4, 1998, pp. 439-455.